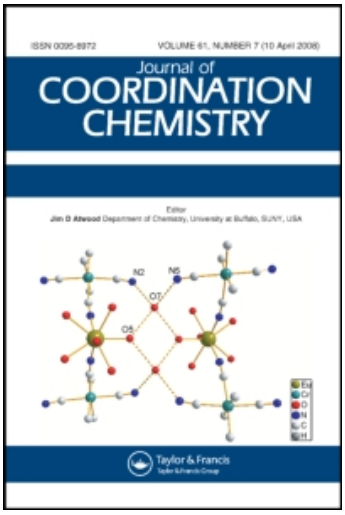

Journal of Coordination Chemistry
Publication details, including instructions for authors and subscription information:
http://www.informaworld.com/smpp/title~content=t713455674

Effect of the ancillary ligands on the binding of ruthenium(II) complexes $[Ru(dmp)_2(MCMIP)]^{2+}$ and $[Ru(dmb)_2(MCMIP)]^{2+}$ with DNA

Yun-Jun Liu[a]; Jian-Feng He[b]; Jun-Hua Yao[c]; Wen-Jie Mei[a]; Fu-Hai Wu[d]; Li-Xin He[a]
[a] School of Pharmacy, Guangdong Pharmaceutical University, Guangzhou 510006, P.R. China [b] College of Chinese Traditional Medicine, Guangzhou University of Chinese Medicine, Guangzhou 510006, P.R. China [c] Instrumentation Analysis and Research Center, Sun Yat-Sen University, Guangzhou 510275, P.R. China [d] School of Public and Health, Guangdong Pharmaceutical University, Guangzhou 510006, P.R. China

First published on: 01 October 2010

To cite this Article Liu, Yun-Jun , He, Jian-Feng , Yao, Jun-Hua , Mei, Wen-Jie , Wu, Fu-Hai and He, Li-Xin(2009) 'Effect of the ancillary ligands on the binding of ruthenium(II) complexes $[Ru(dmp)_2(MCMIP)]^{2+}$ and $[Ru(dmb)_2(MCMIP)]^{2+}$ with DNA', Journal of Coordination Chemistry, 62: 4, 665 — 675, First published on: 01 October 2010 (iFirst)
To link to this Article: DOI: 10.1080/00958970802266904
URL: http://dx.doi.org/10.1080/00958970802266904

Journal of Coordination Chemistry
Vol. 62, No. 4, 20 February 2009, 665–675

Effect of the ancillary ligands on the binding of ruthenium(II) complexes $[Ru(dmp)_2(MCMIP)]^{2+}$ and $[Ru(dmb)_2(MCMIP)]^{2+}$ with DNA

YUN-JUN LIU*†, JIAN-FENG HE‡, JUN-HUA YAO§, WEN-JIE MEI†, FU-HAI WU¶ and LI-XIN HE†

†School of Pharmacy, Guangdong Pharmaceutical University, Guangzhou, 510006, P.R. China
‡College of Chinese Traditional Medicine, Guangzhou University of Chinese Medicine, Guangzhou, 510006, P.R. China
§Instrumentation Analysis and Research Center, Sun Yat-Sen University, Guangzhou, 510275, P.R. China
¶School of Public and Health, Guangdong Pharmaceutical University, Guangzhou, 510006, P.R. China

(*Received 3 January 2008; in final form 21 April 2008*)

Two polypyridine ruthenium(II) complexes, $[Ru(dmp)_2(MCMIP)]^{2+}$ (**1**) (MCMIP = 2-(6-methyl-3-chromonyl)imidazo[4,5-*f*][1,10]-phenanthroline, dmp = 2,9-dimethyl-1,10-phenanthroline) and $[Ru(dmb)_2(MCMIP)]^{2+}$ (**2**) (dmb = 4,4′-dimethyl-2,2′-bipyridine), have been synthesized and characterized by elemental analysis, ES-MS and ^1H NMR. The DNA-binding behaviors of these complexes were investigated by electronic absorption titration, fluorescence spectroscopy, viscosity measurements and thermal denaturation. The results show that **1** and **2** effectively bind to CT-DNA; the DNA-binding affinities are closely related to the ancillary ligand.

Keywords: Effect of ancillary ligands; Ruthenium(II) complex; DNA

1. Introduction

A number of transition metal complexes have been utilized to probe nucleic acid structure and in the development of DNA-cleaving agents, DNA photoprobes and DNA-molecular light switches [1–9]. Metal complex-DNA associations are induced by weak non-covalent forces, e.g. intercalation (π–π stacking) of ligand between DNA base pairs, van der Waals contacts, hydrogen bonds, hydrophobic interactions and electrostatic interactions [1, 10]. Many applications require complex interacting with DNA through intercalation. Despite considerable literature on metal complex-DNA interactions, the binding of these complexes to DNA and their binding geometries have

*Corresponding author. Email: lyjche@163.com

Journal of Coordination Chemistry
ISSN 0095-8972 print/ISSN 1029-0389 online © 2009 Taylor & Francis
DOI: 10.1080/00958970802266904

remained a subject of debate [11]. The binding of $[Ru(phen)_3]^{2+}$ remains an issue of rigorous debate [12, 13] with factors such as size, shape and planarity of the intercalative ligand, and changing substituent group or substituent position on the intercalative ligand influencing the DNA-binding mechanism [9, 14–16]. In contrast, investigations on the influence of the ancillary ligands of Ru(II) complexes have been few. Since octahedral polypyridine Ru(II) complexes bind to DNA in three dimensions, the ancillary ligands also play an important role in the DNA-binding mechanism and behaviors. Barton *et al.* [17, 18] reported that $[Rh(MGP)_2phi]^{5+}$ (MGP = 4-(guanidylmethyl)-1,10-phenanthroline, phi = phenanthrenequinone diimine) and $[Rh(GEB)_2phi]^{5+}$ (GEB = 4-(2-guanidylethyl)-4′-methyl-2,2′-bipyridine) show different sequence recognition, different DNA-binding affinities and cleavage due to the different ancillary ligand. The Ru(II)-dppz (dppz = dipyrido[3,2-a: 2′,3′-c]-phenazine) complexes with different ancillary ligands e.g. bpy(2,2′-bipyridine), phen(1,10-phenanthroline), dmb and dmp can display different DNA-binding affinities and sequence specificity [19–21]. Therefore, it is significant to find the effect of ancillary ligand on the interaction and binding of these complexes to DNA. In this article, we describe the synthesis, characterization and DNA-binding of two new ruthenium(II) mixed-ligand complexes, $[Ru(dmp)_2(MCMIP)]^{2+}$ (**1**) (MCMIP = 2-(6-methyl-3-chromonyl)imidazo [4,5-*f*][1,10]-phenanthroline, dmp = 2,9-dimethyl-1,10-phenanthroline) and $[Ru(dmb)_2(MCMIP)]^{2+}$ (**2**) (dmb = 4,4′-dimethyl-2,2′-bipyridine). Their DNA-binding behaviors have been investigated by electronic absorption titration, fluorescence spectroscopy, thermal denaturation and viscosity measurements. The experimental results show that **1** and **2** effectively bind to CT-DNA.

2. Experimental

2.1. *Materials*

Calf thymus DNA (CT-DNA) was obtained from the Sino-American Biotechnology Company. Doubly-distilled water was used to prepare buffers (5 mM *tris*(hydroxymethylaminomethane)-HCl, 50 mM NaCl, pH = 7.2); dmp and dmb were purchased from Guangzhou Chemical Reagent Factory. 3-Formyl-6-methylchromone was purchased from Aldrich Chemicals. All other chemicals were of analytical reagent grade and used without purification.

2.2. *Physical measurements*

Microanalysis (C, H, and N) was carried out with a Perkin-Elmer 240Q elemental analyzer. Electrospray mass spectra (ES-MS) were recorded on a LCQ system (Finnigan MAT, USA) using methanol as mobile phase. The spray voltage, tube lens offset, capillary voltage and capillary temperature were set at 4.50 KV, 30.00 V, 23.00 V and 200°C, respectively, and the quoted m/z values are for the major peaks in the isotope distribution. ^{1}H NMR spectra were recorded on a Varian-500 spectrometer. All chemical shifts are relative to tetramethylsilane (TMS). UV–Vis spectra were recorded on a Shimadzu UV-3101PC spectrophotometer at room temperature.

Cyclic voltammetric measurements were performed on a CHI 660A Electrochemical Workstation. All samples were purged with nitrogen prior to measurements. A standard three-electrode system comprised of a platinum microcylinder working electrode, platinum-wire auxiliary electrode and a saturated calomel reference electrode (SCE) was used.

2.3. *DNA binding studies*

All experiments involving interaction of the complexes with DNA were conducted in *Tris*-HCl buffer. A solution of calf thymus DNA in the buffer gave a ratio of UV absorbance at 260 and 280 nm of ca. 1.8–1.9 : 1, indicating that the DNA was sufficiently free of protein [22]. The DNA concentration per nucleotide was determined by absorption spectroscopy using the molar absorption coefficient ($6600\,M^{-1}\,cm^{-1}$) at 260 nm [23].

The absorption titration experiment was performed by maintaining the ruthenium(II) complex concentration (20 μM) and varying the concentration of nucleic acid from 14 to 210 μM. Ruthenium-DNA solutions were allowed to incubate for 5 min before measuring the absorption spectra; equal amount of DNA was added to both complex solution and the reference solution to eliminate the absorbance of DNA itself. The intrinsic binding constant K_b with CT-DNA was obtained by monitoring the change in absorbance of the metal-to-ligand transfer (MLCT), with increasing concentration of DNA. The intrinsic binding constants K_b of Ru(II) complexes to DNA were determined from equation (1) [24].

$$\frac{[DNA]}{\varepsilon_a - \varepsilon_f} = \frac{[DNA]}{\varepsilon_b - \varepsilon_f} + \frac{1}{K_b(\varepsilon_b - \varepsilon_f)} \tag{1}$$

where [DNA] is the concentration of DNA in base pairs, ε_a, ε_f and ε_b correspond to the apparent absorption coefficient $A_{obsd}/[Ru]$, the extinction coefficient for the free ruthenium complex and the extinction coefficient for the ruthenium complex in the fully bound form, respectively. In plots of $[DNA]/(\varepsilon_a - \varepsilon_f)$ *versus* [DNA], K_b is given by the ratio of slope to the intercept.

Viscosity measurements were carried out using an Ubbelodhe viscometer maintained at 28.0 (±0.1)°C in a thermostated bath. DNA samples of approximately 200 base pairs in average length were prepared by sonicating in order to minimize complexities arising from DNA flexibility [25]. Flow time was measured with a digital stopwatch, each sample was measured three times, and an average flow time was calculated. Data were presented as $(\eta/\eta_0)^{1/3}$ *versus* binding ratio [26], where η is the viscosity of DNA in the presence of complex and η_0 is the viscosity of DNA alone.

Thermal denaturation studies were carried out with a Perkin-Elmer Lambda 35 spectrophotometer equipped with a Peltier temperature-controlled programmer (±0.1°C). The melting curves were obtained by measuring the absorbance at 260 nm for solutions of CT-DNA (80 μM) in the absence and presence of different Ru(II) complex as a function of temperature. The temperature was scanned from 50 to 90°C at a speed of $1°C\,min^{-1}$. The melting temperature (T_m) was taken as the mid-point of the hyperchromic transition.

2.4. *Preparation of complexes*

2.4.1. [Ru(dmp)$_2$(MCMIP)](ClO$_4$)$_2$ (1). A mixture of *cis*-[Ru(dmp)$_2$Cl$_2$]·2H$_2$O [27] (0.312 g, 0.5 mmol) and MCMIP [28] (0.189 g, 0.5 mmol) in ethylene glycol (20 cm^3) was heated at 120°C under argon for 8 h to give a clear red solution. Upon cooling, a red precipitate was obtained by dropwise addition of saturated aqueous $NaClO_4$ solution. The crude product was purified by column chromatography on neutral alumina with a mixture of CH_3CH-toluene (3 : 1, v/v) as eluant. The mainly red band was collected. The solvent was removed under reduced pressure and a red powder was obtained. Yield: 63%. Anal. Found: C, 55.93; H, 3.54; N, 10.21%. Calcd for $C_{51}H_{38}N_8Cl_2O_{10}Ru$: C, 55.95; H, 3.50; N, 10.23%. ES-MS [CH_3CN, m/z]: 994.9 ([M−ClO$_4$]$^+$), 895.1 ([M−2ClO$_4$−H]$^+$), 448.2 ([M−2ClO$_4$]$^{2+}$). ^{1}H NMR (500 MHz, DMSO-d$_6$): δ 9.25 (s, 1H), 8.92 (d, 2H, $J = 8.7$ Hz), 8.44 (t, 4H), 8.25 (d, 2H, $J = 8.6$ Hz), 8.06 (s, 4H), 7.99 (d, 2H, $J = 8.5$ Hz), 7.72 (t, 1H), 7.53 (t, 2H), 7.40 (d, 4H, $J = 8.4$ Hz), 3.28 (s, 3H), 2.51 (s, 12H).

2.4.2. [Ru(dmb)$_2$(MCMIP)](ClO$_4$)$_2$ (2). This complex was synthesized in a manner identical to that described for **1**, with *cis*-[Ru(dmb)$_2$Cl$_2$]·2H$_2$O [29] in place of *cis*-[Ru(dmp)$_2$Cl$_2$]·2H$_2$O. Yield: 65%. Anal. Found: C, 53.94; H, 3.69; N, 10.68. Calcd for $C_{47}H_{38}N_8Cl_2O_{10}Ru$: C, 53.93; H, 3.66; N, 10.70%. ES-MS [CH_3CN, m/z]: 947.0 ([M−ClO$_4$]$^+$), 847.1 ([M−2ClO$_4$−H]$^+$), 424.3 ([M−2ClO$_4$]$^{2+}$). ^{1}H NMR (500 MHz, DMSO-d$_6$): δ 9.46 (d, 1H, $J = 8.5$ Hz), 9.34 (s 1H), 9.04 (d, 1H, $J = 8.5$), 8.72 (d, 4H, $J = 8.0$), 8.29 (s, 4H), 8.06 (d, 2H, $J = 8.6$ Hz), 7.91 (d, 1H, $J = 8.2$ Hz), 7.74–7.79 (m, 2H), 7.66 (d, 1H, $J = 7.6$ Hz), 7.42 (d, 4H, $J = 7.8$ Hz), 7.16 (d, 1H, $J = 8.0$ Hz), 3.26 (s, 3H), 2.57 (s, 12H).

3. Results and discussion

3.1. *Synthesis and characterization*

MCMIP was synthesized on the basis of the method for imidazole ring preparation established by Steck *et al.* [30]. The complexes were synthesized by direct reaction of MCMIP with *cis*-[Ru(dmp)$_2$Cl$_2$]·2H$_2$O or *cis*-[Ru(dmb)$_2$Cl$_2$]·2H$_2$O in ethylene glycol in relatively high yield. The desired ruthenium(II) complexes were isolated as the perchlorates and purified by column chromatography.

In the ES-MS spectra for the Ru(II) complexes, all of the expected signals [M−ClO$_4$]$^+$, [M−2ClO$_4$−H]$^+$ and [M−2ClO$_4$]$^{2+}$ were observed. Complexes **1** and **2** give well-defined ^{1}H NMR spectra (figure 1) and different protons were assigned by analogy [28]. A full assignment was made for the multiples in the regions from 6.80 to 9.50 ppm. The proton resonance on the nitrogen atom of the imidazole ring of MCMIP was not observed because the proton exchanges quickly between the two nitrogens of the imidazole ring. Similar examples have been reported previously [31, 32].

The absorption spectra of **1** and **2** are shown in table 1 and characterized by intense π–π^* ligand transition in the UV and metal-to-ligand charge transfer (MLCT) transition in the visible region. The bands at 467 and 464 nm are assigned to the metal-to-ligand charge transfer (MLCT) transition. The bands below 300 nm are attributed to

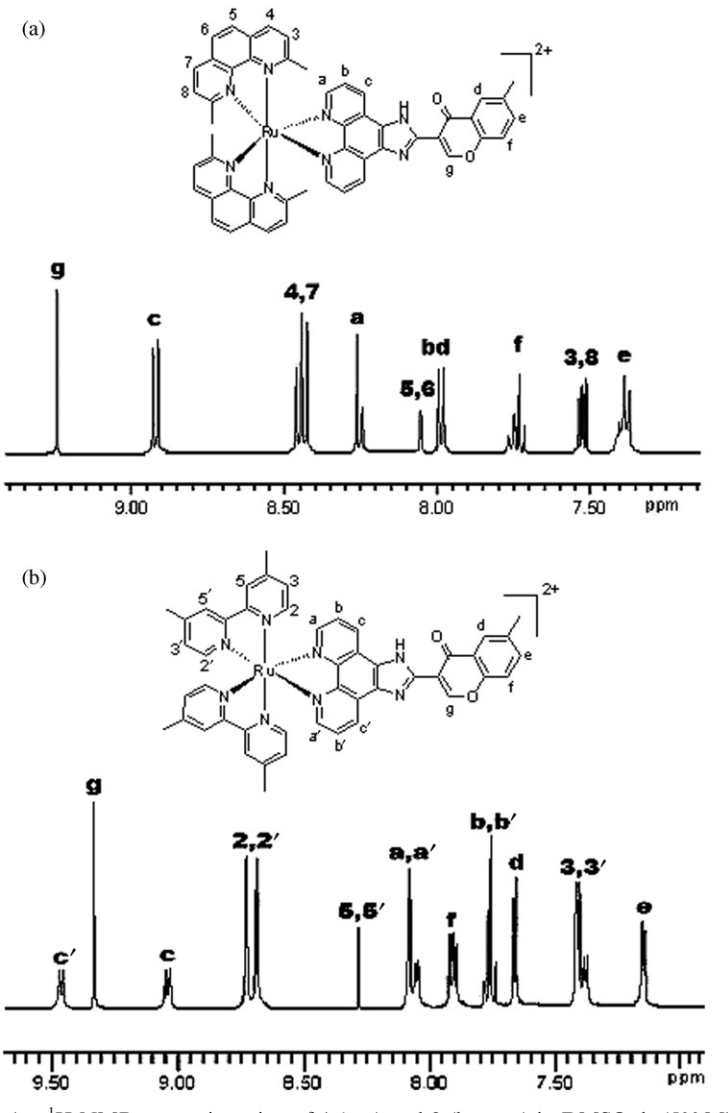

Figure 1. ^{1}H NMR aromatic region of **1** (top) and **2** (bottom) in DMSO-d_6 (500 MHz).

intraligand (IL) transition by comparison with the spectrum of other polypyridine Ru(II) complexes [31, 32].

The electrochemical behavior of the two complexes were examined in acetonitrile. Each complex exhibits one oxidation and three reduction waves in the sweep range from −2.0 to +2.0 V (table 1). An oxidation wave corresponding to the Ru^{III}/Ru^{II} couple was observed at 1.43 and 1.25 V for **1** and **2** (*versus* SCE), respectively. Comparing the oxidation potential of **2** with that of $[Ru(phen)_3]^{2+}$ (1.40 V) [33], **2** loses an electron more easily than $[Ru(phen)_3]^{2+}$. With reference to previous studies [32, 34, 35], the first reduction, which is usually controlled by the ligand having the lowest unoccupied molecular orbital (LUMO), is assigned to a reduction centered on MCMIP and the last two reductions are characteristic of the co-ligand (dmp or dmb).

Table 1. Electrochemical and absorption data of the ruthenium(II) complexes.

Complex	$E_{1/2}$(V) *vs.* SCE[a]				λ_{max}/nm[b] (ε dm^{-3} mol^{-1} cm^{-1})
	RuII/III	Ligand	Reduction		
$[Ru(phen)_3]^{2+}$	1.40	−1.41	−1.54	−1.84	
1	1.43	−0.80	−1.37	−1.61	469 (14515), 273 (78512)
2	1.25	−0.82	−1.43	−1.64	465 (10728), 285 (59976)

[a]All data were measured in 0.1 M NBu_4ClO_4–MeCN, error in potentials was ±0.02 V; scan rate = 100 mVS^{-1}.
[b]In CH_3CN.

3.2. *Electronic titration studies*

The application of electronic absorption spectroscopy in DNA-binding studies is one of the most powerful experimental techniques for probing metal ion-DNA interaction. Binding of the macromolecule leads to changes in the electronic spectrum of the metal complex. Base binding is expected to perturb the ligand field transition of the metal complex [11]. Due to the intercalative mode involving a strong stacking interaction between an aromatic chromophore and the base pairs of DNA, complex binding with DNA through intercalation usually results in hypochromism and bathochromism; the extent of the hypochromism on the metal-to-ligand charge transfer (MLCT) commonly parallels the intercalative binding strength. The absorption spectra of **1** and **2** at 25°C in the absence and presence of CT-DNA are given in figure 2. For **1**, the intensities of the intraligand band at 271 nm decrease with increasing concentration of DNA. The band at 467 nm (MLCT band) is red shifted by 4 nm and the hypochromism reaches as high as 14.5%. In the case of **2**, the intensity of the intraligand band at 283 nm also decreases in the presence of DNA; the hypochromism at 464 nm (MLCT band) was observed to be 17.8%. These spectral characteristics suggest that the two complexes interact with DNA most likely through intercalation. The DNA-binding constants of **1** and **2** have been determined to be 5.42×10^3 M^{-1} and 2.25×10^4 M^{-1}, respectively. Due to less π-conjugated aromatic area, these values are less than those of classical intercalators, such as $[Ru(bpy)_2(dppz)]^{2+}$ (dppz = dipyrido-[3,2-a:2′,3′-c]phenazine, $K > 10^6$) [36] and $[Ru(bpy)_2(ppd)]^{2+}$ (ppd = pteridino [7,6-*f*][1,10]phenanthroline-1,13-(10*H*,12*H*)-dione, $K = 1.3 \times 10^6$) [37]. The difference between the two intrinsic constants is from different ancillary ligands. Complex **1** shows the least binding strength to double-helical DNA. Substitution on the 2- and 9-positions of the ancillary phen ligands must cause severe steric constraints near the core of Ru(II) when the complex intercalates into the DNA base pairs. The methyl groups may come into close proximity of base pairs at the intercalation sites. These steric clashes then prevent the complex from intercalating effectively, decreasing the intrinsic constant. Such clashes would not be present with substitution on the 4- and 4′-positions of the ancillary bpy ligands [19]. The results show that the DNA binding affinities of these complexes closely correlate to the effects of ancillary ligands.

3.3. *Luminescence studies*

The emission intensities of complexes from their MLCT excited state are found to depend on DNA concentration. The emission spectra of complexes in the absence and

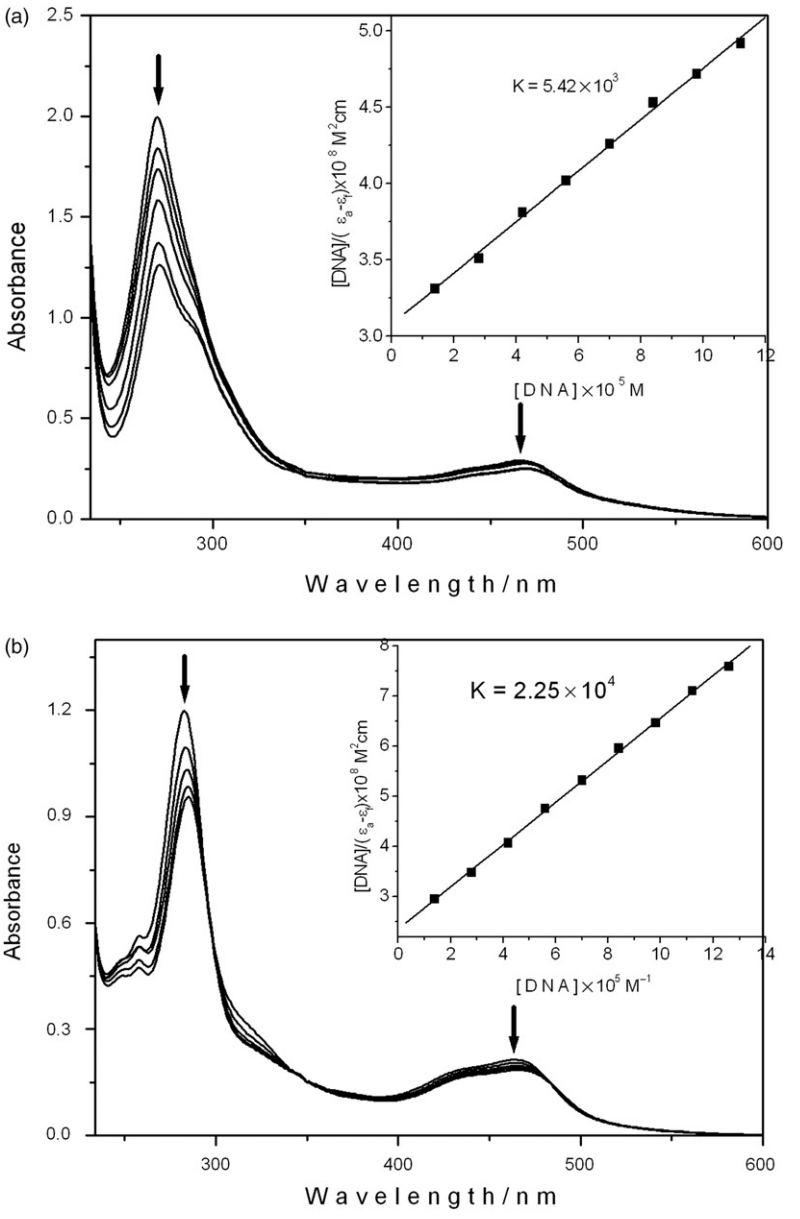

Figure 2. Absorption spectra of complexes in *Tris*-HCl buffer upon addition of CT-DNA in the presence of **1** (a) and **2** (b). [Ru] = 20 μM. Arrow shows the absorbance changing upon the increase of DNA concentration. Plots of $(\varepsilon_a-\varepsilon_f)/(\varepsilon_b-\varepsilon_f)$ *vs*. [DNA] for the titration of DNA with Ru(II) complexes.

presence of calf thymus DNA are shown in figure 3. In the absence of DNA, **1** and **2** can emit luminescence in *Tris* buffer at ambient temperature, with maxima appearing at 609 and 607 nm for **1** and **2**, respectively. Upon addition of DNA, the emission intensities of **1** and **2** increase to 3.53 and 3.72 times larger than the original, respectively. The enhancement of emission intensity is indicative of binding of the complexes to the hydrophobic pocket of DNA, efficiently protected by DNA.

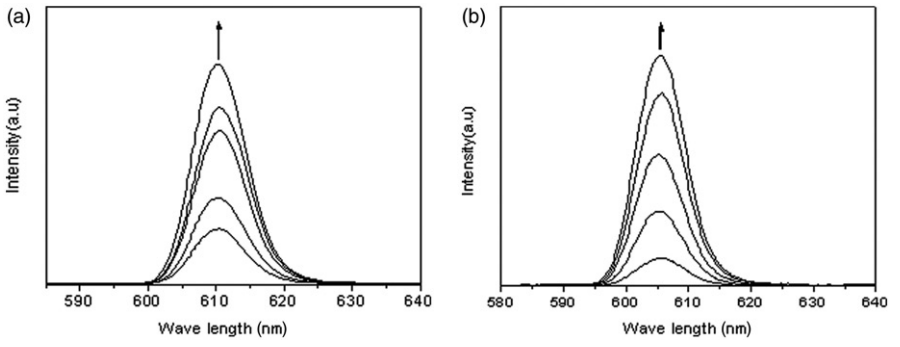

Figure 3. Emission spectra of **1** (a) and **2** (b) in *Tris*-HCl buffer in the absence and presence of CT-DNA. Arrow shows the intensity change upon increasing DNA concentrations.

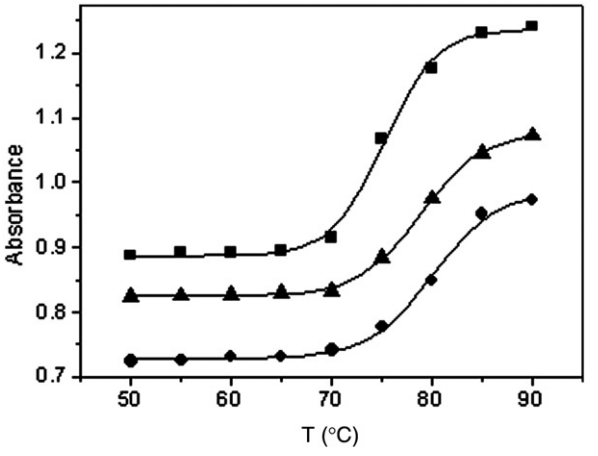

Figure 4. Thermal denaturation of calf thymus DNA in the absence (■) and presence of **1** (▲) and **2** (●). [Ru] = 20 μM, [DNA] = 80 μM.

3.4. *Thermal denaturation*

When the temperature in solution increases, the double stranded DNA gradually dissociates to single strands and generates a hypochromic effect on absorption spectra of DNA bases ($\lambda_{max} = 260$ nm). The melting temperature T_m, which is defined as the temperature where half of the total base pairs are unbonded, is determined from the thermal denaturation curves of DNA. Generally, the melting temperature increases when metal complexes bind to DNA by intercalation. As intercalation of the complexes into DNA base pairs causes stabilization of base stacking and hence raises the melting temperature of the double-stranded DNA, DNA melting experiments are useful in establishing the extent of intercalation [38]. In the presence of intercalators, the T_m rises sharply with low intercalator concentration until all intercalation sites are saturated, after which stabilization is due to electrostatic binding and T_m increases less steeply. Figure 4 shows, in the absence of **1** and **2**, the T_m of CT-DNA was 75.2 ± 0.5°C; the melting point increased by 3.7 and 4.9°C for **1** and **2** at a concentration ratio of

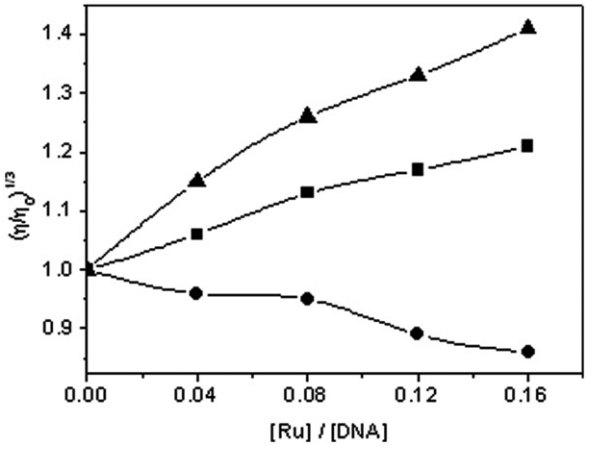

Figure 5. Effect of increasing amounts of ethidium bromide (▲), **1** (●) and **2** (■) on the relative viscosity of calf thymus DNA at 28 (±0.1)°C. [DNA] = 0.5 mM.

[Ru]/[DNA] = 1 : 5. These values clearly show that **2** stabilizes the DNA helix more than **1**, consistent with **2** binding to DNA more strongly than **1** as revealed by their DNA-binding constants.

3.5. *Viscosity measurements*

To further clarify interactions between the complex and DNA, viscosity measurements were carried out. Optical photophysical probes provide necessary but not sufficient clues to support a binding mode. Viscosity measurements that are sensitive to length change of DNA are regarded as the least ambiguous and most critical test of binding mode in solution in the absence of crystallographic structural data or NMR spectra [12, 39]. A classical intercalation mode results in lengthening the DNA helix, as base pairs are separated to accommodate the binding ligand, leading to increase of DNA viscosity. In contrast, a partial and/or non-classical intercalation of ligand could bend (or kink) the DNA helix, reduce its effective length and, concomitantly, its viscosity [12, 39]. The effects of **1** and **2**, together with ethidium bromide (EB) on the viscosity of rod-like DNA, are shown in figure 5. EB, a known DNA intercalator, increases the relative specific viscosity via lengthening of the DNA double helix resulting from intercalation. On increasing the amount of **2**, the relative viscosity of DNA increases from 1.0 to 1.21, similar to the behavior of ethidium bromide. However, the relative viscosity of DNA decreases from 1.0 to 0.86 upon increasing the amounts of **1**, which indicates that **1** interacts with DNA through partial intercalation.

4. Conclusion

Two mixed-ligand polypyridine complexes, $[Ru(dmp)_2(MCMIP)]^{2+}$ and $[Ru(dmb)_2(MCMIP)]^{2+}$, have been synthesized and characterized by elemental analysis, ES-MS

and ^{1}H NMR. Both complexes show hypochromism in the MLCT band in the presence of DNA and binding constants have been determined through spectroscopic titration. Relative viscosity of DNA has been found to increase in the presence of **2**, whereas the relative viscosity of DNA decreases in the presence of **1** due to the severe steric constraints of 2,9-dimethyl-1,10-phenanthroline (dmp). The results indicate that the two complexes bind to CT-DNA, and the DNA-binding affinities are related to the ancillary ligand.

Acknowledgements

We are grateful to the Nature Science Foundation of Guangdong Province (No. 0711220400121), the Science and Technology Foundation of Guangdong Province (No. 2004B33301029) and Guangdong Pharmaceutical University for financial support.

References

[1] K.E. Erkkila, D.T. Odem, J.K. Barton. *Chem. Rev*., **99**, 2777 (1999).
[2] C. Metcalfe, J.A. Thomas. *Chem. Soc. Rev*., **32**, 215 (2003).
[3] P.U. Maheswari, M. Palaiandavar. *J. Inorg. Biochem*., **98**, 219 (2004).
[4] A.E. Friedman, J.C. Chambron, J.P. Sauvage, N.J. Turro, J.K. Barton. *J. Am. Chem. Soc*., **112**, 4960 (1990).
[5] V.W.W. Yam, K.K.W. Lo, K.K. Cheung, R.Y.C. Kong. *Dalton Trans*., 2067 (1997).
[6] H.D. Stoeffler, N.B. Thornton, S.L. Temkin, K.S. Schanze. *J. Am. Chem. Soc*., **117**, 7119 (1995).
[7] C. Metcalfe, M. Webb, J.A. Thomas. *Chem. Commun*., 2026 (2002).
[8] S. Arounaguiri, B.G. Maiya. *Inorg. Chem*., **38**, 842 (1999).
[9] X.W. Liu, J. Li, H. Li, K.C. Zheng, H. Chao, L.N. Ji. *J. Inorg. Biochem*., **99**, 2372 (2005).
[10] C.S. Chow, F.M. Bogdan. *Chem. Rev*., **97**, 1489 (1997).
[11] D. Lawrence, V.G. Vaidyanathan, U.N. Balachandran. *J. Inorg. Biochem*., **100**, 1244 (2006).
[12] S. Satyanarayana, J.C. Dabrowiak, J.B. Chaires. *Biochemistry*, **32**, 2573 (1993).
[13] J.E. Coury, J.R. Anderson, L. McFail-Isom, L.D. Williams, L.A. Battenly. *J. Am. Chem. Soc*., **119**, 3792 (1997).
[14] Y.J. Liu, X.Y. Wei, W.J. Mei, L.X. He. *Transition Met. Chem*., **32**, 762 (2007).
[15] L.F. Tan, H. Chao. *Inorg. Chim. Acta*, **360**, 2016 (2007).
[16] J.G. Liu, B.H. Ye, H. Li, Q.X. Zhen, L.N. Ji. *J. Inorg. Biochem*., **76**, 265 (1999).
[17] R.H. Terbrueggen, T.W. Johann, J.K. Barton. *Inorg. Chem*., **37**, 6874 (1998).
[18] S.J. Franklin, J.K. Barton. *Biochemistry*, **37**, 16093 (1998).
[19] J.G. Liu, Q.L. Zhang, X.F. Shi, L.N. Ji. *Inorg. Chem*., **40**, 5045 (2001).
[20] P.U. Maheswari, V. Rajendiran, M. Palaniandavar, R. Parthasarathi, V. Subramanian. *J. Inorg. Biochem*., **100**, 3 (2006).
[21] T. Biver, C. Cavazza, F. Secco, M. Venturini. *J. Inorg. Biochem*., **101**, 461 (2007).
[22] J. Marmur. *J. Mol. Biol*., **3**, 208 (1961).
[23] M.F. Reichmann, S.A. Rice, C.A. Thomas, P. Doty. *J. Am. Chem. Soc*., **76**, 3047 (1954).
[24] A. Wolf, G.H. Shimer Jr, T. Meehan. *Biochemistry*, **26**, 6392 (1987).
[25] J.B. Chaires, N. Dattagupta, D.M. Crothers. *Biochemistry*, **21**, 3933 (1982).
[26] G. Cohen, H. Eisenberg. *Biopolymers*, **8**, 45 (1968).
[27] J.P. Collin, T.P. Sauvage. *Inorg. Chem*., **25**, 135 (1986).
[28] Y.J. Liu, H. Chao, Y.X. Yuan, H.J. Yu, L.N. Ji. *Inorg. Chim. Acta*, **359**, 3807 (2006).
[29] B.P. Sullivan, D.J. Salmon, T.J. Meyer. *Inorg. Chem*., **17**, 3334 (1978).
[30] E.A. Steck, A.R. Day. *J. Am. Chem. Soc*., **65**, 452 (1943).
[31] J.Z. Wu, B.H. Ye, L. Wang, L.N. Ji, J.Y. Zhou, R.H. Li. *J. Chem. Soc., Dalton Trans*., 1395 (1997).
[32] L.F. Tan, H. Chao, Y.F. Zhou, L.N. Ji. *Polyhedron*, **26**, 3029 (2007).
[33] B.K. Ghosh, A. Chkravorty. *Coord. Chem. Rev*., **95**, 239 (1989).

[34] T. Matsumura-Inoue, H. Tomoro, M. Kasai, T. Tominiga-Morimoto. *J. Electroanal. Chem.*, **95**, 109 (1979).
[35] Y.J. Liu, H. Chao, Y.H. Yao, H. Li, Y.X. Yuan, L.N. Ji. *Helv. Chim. Acta*, **87**, 3119 (2004).
[36] E.J.C. Olson, D. Hu, A. Hormann, A.M. Jonkman, M.R. Arkin, E.D.A. Stemp, J.K. Barton, P.F. Barbara. *J. Am. Chem. Soc.*, **119**, 11458 (1997).
[37] F. Gao, H. Chao, F. Zhou, Y.X. Yuan, B. Peng, L.N. Ji. *J. Inorg. Biochem.*, **100**, 1487 (2006).
[38] C.V. Kumar, E.H. Asuncion. *J. Am. Chem. Soc.*, **115**, 8547 (1993).
[39] S. Satyanarayana, J.C. Dabrowiak, J.B. Chaires. *Biochemistry*, **31**, 9319 (1992).